energies

MDPI

Article

Energy Efficiency Optimization of Collaborative Power Supply System with Supercapacitor Storages

Yibo Deng [1], Chushan Li [2], Yan Deng [1], Ting Chen [3], Shaoyu Feng [3], Yujie Chu [3] and Chengmin Li [1,*]

[1] College of Electrical Engineering, Zhejiang University, Hangzhou 310027, China
[2] Zhejiang University–University of Illinois at Urbana–Champaign Institute, Zhejiang University, Hangzhou 310027, China
[3] Ningbo CRRC New Energy Technology Co., Ltd., Ningbo 315112, China
* Correspondence: lichengmin@zju.edu.cn

Abstract: To solve the challenge of low efficiency and high operation cost caused by intermittent high-power charging in an energy storage tram, this work presents a collaborative power supply system with supercapacitor energy storage. The scheme can reduce the peak power of the transformer, therefore reducing the grid-side capacity and improving the efficiency. However, there is a lack of quantitative analysis on the performance improvement of the solution. The energy efficiency models of critical components are proposed to evaluate the efficiency of the system, and energy efficiency optimization is conducted. Taking an operational tram line as an example, the improved charging efficiency and reduced operating costs are derived. Further, the ground energy storage capacity is designed and implemented. The measured data demonstrates that the energy efficiency of the optimized charging system is improved, which proves its effectiveness and practicability.

Keywords: energy storage; supercapacitor; intermittent power supply system; power supply efficiency

Citation: Deng, Y.; Li, C.; Deng, Y.; Chen, T.; Feng, S.; Chu, Y.; Li, C. Energy Efficiency Optimization of Collaborative Power Supply System with Supercapacitor Storages. *Energies* **2023**, *16*, 1227. https://doi.org/10.3390/en16031227

Academic Editors: Mojtaba Mirzaeian, Peter Hall, Desmond Gibson and Saule Aidarova

Received: 10 December 2022
Revised: 13 January 2023
Accepted: 20 January 2023
Published: 23 January 2023

1. Introduction

With the continuous advancement of urbanization and the sharp increase in urban population, urban road congestion has become increasingly severe, causing great challenges for citizens to travel. There is ever-increasing demand for trams in urban areas. Meanwhile, to realize the carbon neutrality goals, green transportation is among the critical solutions [1–4]. Compared with the traditional overhead catenary-powered trams, the energy storage tram has the following advantages: (1) more than 85% braking energy recovery rate and low operational energy consumption; (2) only the platform area is equipped with a charging rail, without any overhead line visual pollution and transmission loss; (3) no need for backflow through the running track, no electrical corrosion to the underground pipe network; (4) punctuality and fast speed [5–8]. At present, energy storage trams have been successively deployed in commercial operations in China, Spain, and Germany, such as Guangzhou Haizhu, Jiangsu Huaian, Shenzhen Longhua, Wuhan Dahanyang, Seville,Zaragoza, and Mannheim [8–11]. To realize a short time ($\leq$30 s) electric energy replenishment of the energy-storage tram, an MW-level high-power charging system is required to ensure uninterrupted operation of the vehicle.

Supercapacitors have a series of benefits including high power density (2~15 kW/kg), long cycle life (10^5 to 10^6 times), wide operating temperature window (−40~+70 °C), and high energy conversion efficiency ($\geq$90%) [3]. Therefore, supercapacitors have been utilized as the power supply for energy storage trams, the ground energy storage system for regenerative braking energy, and the auxiliary starting device for internal combustion engines.

A series of high-power charging system schemes for supercapacitors have been proposed in recent years [12–18]. The priority is to focus on the optimal design of safety, stability, efficiency, and ripple of the charging system. In [19], the two-stage conversion

of the PWM rectifier and BUCK converter are used to realize the design of a 2 MW charging device in a parallel connection. In [20], a two-stage circuit topology is proposed, in which the front-stage DC/DC converter is boosted and the back-stage DC/DC converter is stepped down. The power feedforward of the post-stage converter is controlled to the pre-stage converter to stabilize the DC bus voltage. Thus, the obtained voltage range can meet the charging requirements of the supercapacitor. In [21], a zero-voltage switching (ZVS) phase-shifted full-bridge module with multiple parallel isolation topologies is proposed. It has the advantages of good security, great output voltage stability, high charging efficiency, and a small ripple coefficient.

Moreover, the optimal design of the power supply system and on-board supercapacitors are drawing attention. The power supply system of the supercapacitor energy storage tram is further analyzed from the external power supply, traction load characteristics, main wiring form, and operation mode [22]. In addition, the design scheme of the off-grid power supply system is obtained. It mainly includes three types: single-unit one-to-one type, single-unit one-to-many type, and double-unit one-to-many type.

However, the platform power supply system of the energy storage tram is still connected by high voltage, and then the vehicle is charged through voltage step-down transformer and rectification stage. The drawbacks of the solution include the large connection capacity (based on peak power), high no-load loss, and high grid current distortion. Moreover, when the power distribution network is in fault or disconnected, the power supply will be terminated, resulting in operation failure. In order to increase the service life of trams, reduce the capacity dependence on the power grid, and reduce operation cost, it is necessary to further upgrade the power supply architecture. It has been studied and discussed separately in existing works about the power supply equipment of the energy storage tram, the charging equipment, and the vehicle operation configuration. However, further insight into the energy efficiency optimization of charging facilities is still missing [23–27].

In this paper, we proposed an energy efficiency optimization design scheme for a collaborative power supply system with supercapacitor energy storage, which is embodied as follows:

(1) The system architecture and efficiency flow block diagram of the collaborative energy storage charging system is proposed;
(2) Based on the main parameters of the on-board supercapacitor, the efficiency of the two charging forms is calculated and analyzed. It can be concluded that the energy storage synergy is feasible to improve energy efficiency;
(3) Finally, the configuration scheme of the supercapacitor energy storage system is implemented and demonstrated in real operation.

2. Module Charging System Architecture

The conventional charging system (i.e., direct charging system) refers to directly charging the vehicles after they enter the stations, and its characteristics of short-time pulse (within 30 s) and high power cause a large no-load loss of the transformer. With the introduction of supercapacitors, the energy storage collaborative charging system can reduce the no-load loss of the transformer and improve the utilization of the transformer capacity. However, the introduction of supercapacitors increases the energy conversion link of the entire charging system. Therefore, it is necessary to study the overall performance. On the basis of satisfying the functional requirements, it is of significance to optimize the efficiency of each link, and ultimately improve the overall efficiency of the charging system.

2.1. Topology of Power Supply System

The topologies of the direct charging system and collaborative energy storage charging system are shown in Figure 1. The direct charging system mainly includes 10 kV distribution network, transformers, rectifiers, step-down DC/DC converters, isolation switches, power supply rails, and connecting cables. Compared with direct charging

system, the collaborative energy storage charging system has a boost DC/DC converter and supercapacitor energy storage devices. In Figure 1a, the transformer parameters are AC 10 kV/900 V 800 kVA; in Figure 1b the transformer parameters are AC 10 kV/400 V 125 kVA. As shown in Figure 2, the main improvements of the collaborative energy storage charging system are as follows:

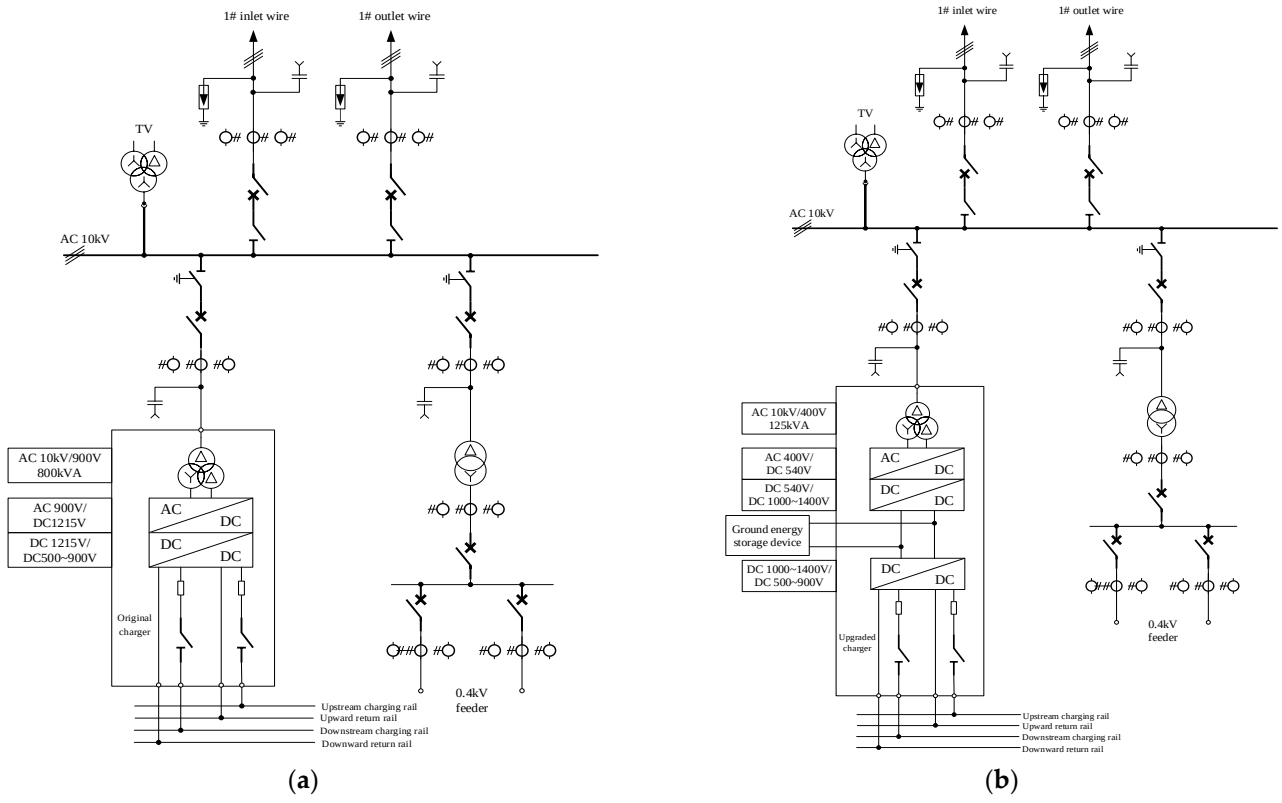

Figure 1. The topology of the charging system. (**a**) Direct charging system. (**b**) Collaborative energy storage system.

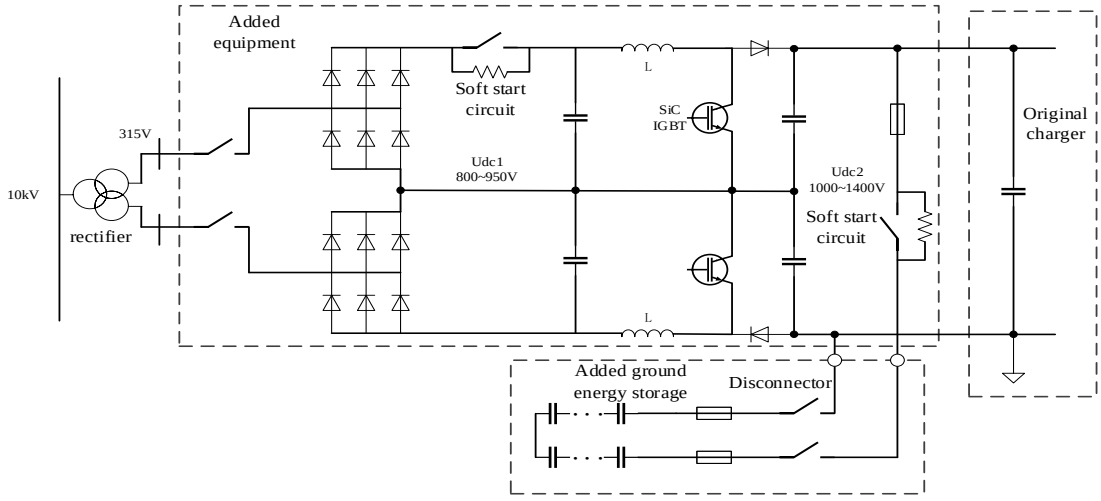

Figure 2. Co-charging topology for supercapacitor energy storage.

(1) The grid voltage of the distribution network is lowered; 10 kV or 0.4 kV power supply can be used for access.
(2) Transformer capacity is reduced. During the operation period, the transformer is able to work under rated conditions, regardless of whether the vehicles are charged or not.

(3) The supercapacitor-based energy storage system supplies power to vehicles when they enter the station, and vice versa.
(4) During the load, power is flattened by energy storage; the boosted DC/DC can work stably under the rated operating conditions, regardless of whether vehicles are charging in the station.

2.2. Efficiency Chain Model of the Charging System

The efficiency flow of the direct charging system is shown in Figure 3, where η_{t0}, η_{r0}, and η_{bk0} represent the transformer efficiency, rectifier efficiency, and step-down DC/DC efficiency of the direct charging system during charging period, respectively. The efficiency flow of the collaborative energy storage charging system during idle period is shown in Figure 4. In Figure 4a, η_{t1}, η_{r1}, η_{bt1}, η_{c1}, and η_{bk1} represent the transformer efficiency, rectifier efficiency, boost DC/DC efficiency, energy storage system charging efficiency, and step-down DC/DC efficiency, respectively. In Figure 4b, η_{t2}, η_{r2}, η_{bt2}, η_{c2}, and η_{bk2} represent the transformer efficiency, rectifier efficiency, boost DC/DC efficiency, energy storage system discharge efficiency, and step-down DC/DC efficiency of the collaborative energy storage charging system during charging period, respectively. In Figures 3 and 4, η_{line} and η_{OESS} indicate the efficiency of distribution network and on-board energy storage system, respectively. Due to the same charging power and time between the direct charging system and collaborative energy storage charging system, $\eta_{bk0} = \eta_{bk2}$ and $\eta_{bk1} = 1$. Since the same working states of the transformer, boost DC/DC, and rectifier during the charging and discharging process are present, $\eta_{t1} = \eta_{t2}$ and $\eta_{r1} = \eta_{r2}$. In analysis, for the sake of simplicity, a fixed efficiency is utilized for loss evaluation of rectifiers, buck DC/DC, and boost DC/DC [28].

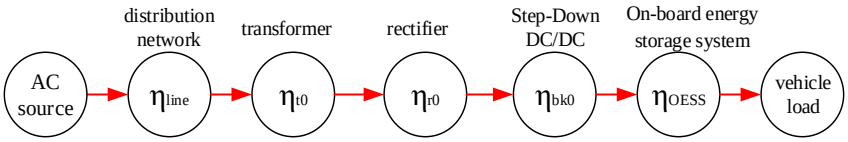

Figure 3. Efficiency flow block diagram of the direct charging system.

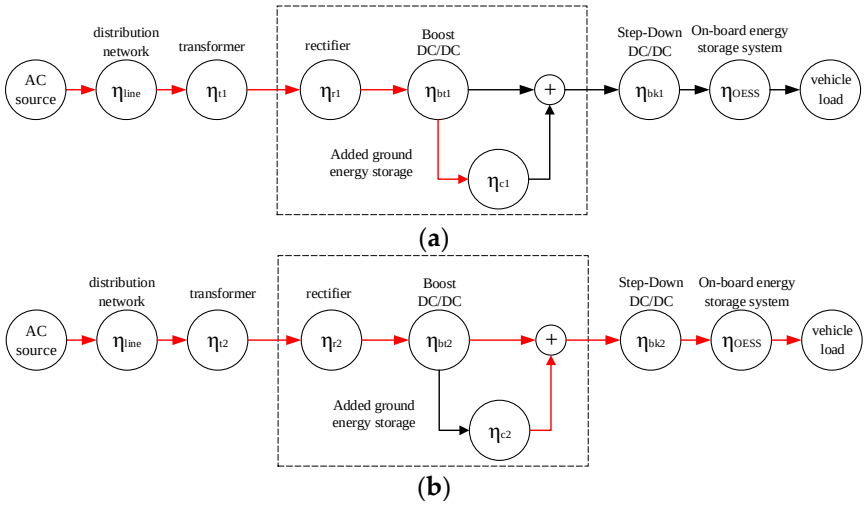

Figure 4. Efficiency flow block diagram of collaborative energy storage charging system. (**a**) Energy storage system charging process. (**b**) Collaborative energy storage system discharge process.

2.3. Load Characteristics Analysis of Charging System

Typically, a charging strategy of "a constant current first and then a constant voltage" is adopted, to complete the charging process in a short time (≤30 s). The main parameters of the on-board supercapacitor energy storage system are shown in Table 1 [29,30].

Table 1. Main technical parameters of on-board supercapacitors.

Parameter	Value
Vehicle marshaling (Car)	4
Capacity (F)	130
Rated voltage (V)	750
Voltage range (V)	500~900
Charging current (A)	1800
Current collection mode	Station stationary charging

The traction load characteristics are shown in Figure 5. The vehicle charging time t_{charge} is $t_2 - t_1$, and the charging interval time t_{interval} is $t_3 - t_2$. The variation of voltage and current with time during supercapacitor charging is shown in Figure 6.

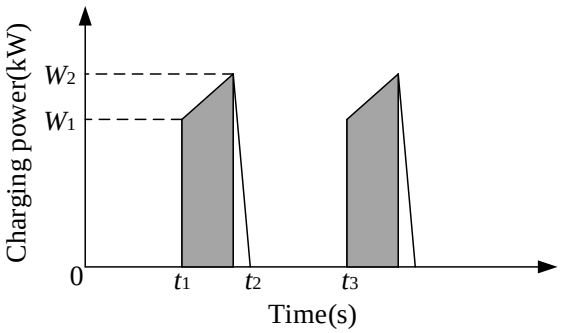

Figure 5. Traction load characteristics.

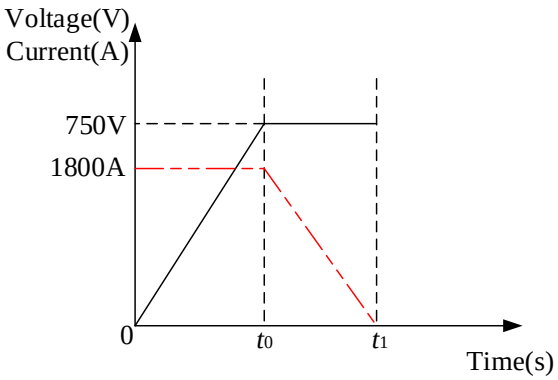

Figure 6. Supercapacitor charging curve.

3. Case Analysis

The system is calculated according to a station in the previous literature [8,9]. The main technical parameters are shown in Table 2. The transformer is 10 kV/0.4 kV 125 kVA; the efficiency of the diode rectifier is 99% (including line loss); and the efficiency of the boost DC/DC converter is 99.2%.

Table 2. The main technical parameters.

Device	Parameter
Input voltage	Three-phase AC 10 kV (−15~+7%)
Input voltage harmonics	≤3% (31 times or less)
Input power factor	Specified load ≥ 0.95, No load ≥ 0.90
Transformer rated power	125 kVA
Charging method	Constant current, limited voltage, and constant power
Output charging voltage	500~900 V
Output power	Total output power ≤ 700 kW and the current can be adjusted according to the operating conditions
Working form	Continuous uninterrupted work

3.1. Calculation of Power System Efficiency

The operating energy consumption of a train station is different in four seasons, with the lowest in winter, medium in spring and autumn, and the highest in summer. Table 3 shows the energy consumption demands of station charging in four seasons of the Haizhu Line.

Table 3. The energy consumption demands of station charging in four seasons.

Season	Summer	Autumn
Traction energy consumption (kWh)	3.0	3.0
Auxiliary energy consumption (kWh)	3.0	2.0
Charging energy consumption (kWh)	6.0	5.0

The charging power is directly related to the SOC of the returning train and the charging time. It is calculated according to the sequential charging principle. The stop time of each train is 30 s, and the available charging time is 25 s (excluding the response time). The constant power of 504 kW can meet the requirements. The number of departure pairs is determined as follows: the average daily number on working days is 80, while the average daily total number on rest days is 89.

3.1.1. Direct Charging

In the power supply chain of direct charging, the total efficiency of the 12-pulse diode rectifier and the cables in the station is 99%. The efficiency of the step-down DC/DC module is 98.5%. The no-load loss and load loss are 1.877 kW and 7.946 kW, respectively.

Combined with the demand for charging energy consumption in different seasons and the driving plan of the line, the loss calculation of each link in the constant power charging is shown in Table 4.

Table 4. The loss calculation results.

Season	Workday		Rest Day	
	Sum.	Fal.	Sum.	Fal.
DC/DC daily loss (kWh)	7.31	4.26	8.13	4.74
Rectifier daily loss (kWh)	4.92	2.87	5.48	3.19
Transformer daily loss (kWh)	48.21	46.89	48.56	47.10
Total daily loss (kWh)	60.44	54.03	62.17	55.04
Average daily power supply efficiency (%)	88.82	83.83	89.57	84.98

The weekly average of the daily power supply efficiency is considered in summer and autumn. It can be calculated that the weekly average power supply efficiency in summer is 89.05%, and the average weekly power supply efficiency in autumn is 83.22%. Then the average charging efficiency is 86.14%.

3.1.2. Energy Storage Synergy

For the collaborative energy storage power supply system, the energy efficiency of the supercapacitor is assumed to be η. Combined with the charging energy consumption demand in each season and the driving plan of the line, the loss of each link in constant power (P_{ch}) charging is calculated in the following. The devices parameters of the charging system shown in Table 5 [9,28].

Table 5. The devices parameters of the charging system.

Parameter	Value
Full load power of transformer (kW)	125
No-load loss power of transformer (kW)	0.14
Load loss power of transformer (kW)	1.53
Step-down DC/DC charging efficiency	0.985
Transformer load efficiency	0.9868
Full load efficiency of rectifier	0.99
Boost DC/DC efficiency	0.992

The single charge loss of step-down DC/DC is

$$E_{\text{loss,dd}} = \frac{E_{\text{op}}}{0.985} \times (1 - 0.985) \tag{1}$$

E_{op} is the charging quantity of on-board energy storage system of each pair of vehicles.

The output of the transformer is at specified load in this case, and the load efficiency is 98.68%. Then the loss of a single synergistic power supply is

$$E_{\text{loss,Tv}} = 125\text{kVA} \times \frac{E_{\text{op}}}{P_{\text{ch}}} \times (1 - 0.9868) \tag{2}$$

The loss of the rectifier is

$$E_{\text{loss,Rv}} = 125\text{kVA} \times \frac{E_{\text{op}}}{P_{\text{ch}}} \times 0.9868 \times (1 - 0.99) \tag{3}$$

The loss of boost DC/DC is

$$E_{\text{loss,ddv}} = 125\text{kVA} \times \frac{E_{\text{op}}}{P_{\text{ch}}} \times 0.9868 \times (1 - 0.992) \tag{4}$$

The loss of ground energy storage device is

$$E_{\text{loss,sc}} = \frac{\left(\frac{E_{\text{op}}}{0.985} - 125\text{kVA} \times \frac{E_{\text{op}}}{P_{\text{ch}}} \times 0.9868 \times 0.99 \times 0.992\right)}{\eta} \times (1 - \eta) \tag{5}$$

The energy consumption of the ground energy storage device during a single charge is

$$E_{\text{ch}} = \frac{\left(\frac{E_{\text{op}}}{0.985} - 125\text{kVA} \times \frac{E_{\text{op}}}{P_{\text{ch}}} \times 0.9868 \times 0.99 \times 0.992\right)}{\eta} \tag{6}$$

The loss of boost DC/DC during a single charge is

$$E_{\text{loss,ddc}} = \frac{E_{\text{ch}}}{0.992} \times (1 - 0.992) \tag{7}$$

The loss of the rectifier during a single charge is

$$E_{\text{loss,Rc}} = \frac{E_{\text{ch}}}{0.992 \times 0.99} \times (1 - 0.99) \tag{8}$$

The charge time of a single cycle of the transformer is

$$T_{\text{rech}} = \frac{1}{D_{\text{peak}}} - \frac{E_{\text{op}}}{P_{\text{ch}}} \tag{9}$$

A load of charge during a single cycle is

$$\frac{E_{\mathrm{ch}}}{0.992 \times 0.99 \times T_{\mathrm{rech}}} \tag{10}$$

The loading efficiency of the transformer during charge is

$$\eta_{\mathrm{Tch}} = \frac{\frac{E_{\mathrm{ch}}}{0.992 \times 0.99 \times T_{\mathrm{rech}}}}{\frac{E_{\mathrm{ch}}}{0.992 \times 0.99 \times T_{\mathrm{rech}}} + 0.14 + \left(\frac{E_{\mathrm{ch}}}{0.992 \times 0.99 \times T_{\mathrm{rech}} \times 125\mathrm{kVA}}\right)^2 \times 1.53} \tag{11}$$

The loss of the transformer during a single charge is

$$E_{\mathrm{loss,Tc}} = \frac{E_{\mathrm{ch}}}{0.992 \times 0.99 \times \eta_{\mathrm{Tch}}} \times (1 - \eta_{\mathrm{Tch}}) \tag{12}$$

The no-load loss of the transformer is

$$E_{\mathrm{loss,Tul}} = 0.14\mathrm{kW} \times \left(24\mathrm{h} - \frac{1}{D_{\mathrm{peak}}} \times N_{\mathrm{day}}\right) \tag{13}$$

The N_{day} is the total number of daily departure pairs. In summary, the total daily loss of each link is:

$$\begin{cases} E_{\mathrm{loss,dd,day}} = E_{\mathrm{loss,dd}} \times N_{\mathrm{day}} \\ E_{\mathrm{loss,sc,day}} = E_{\mathrm{loss,sc}} \times N_{\mathrm{day}} \\ E_{\mathrm{loss,boost,day}} = (E_{\mathrm{loss,ddv}} + E_{\mathrm{loss,ddc}}) \times N_{\mathrm{day}} \\ E_{\mathrm{loss,R,day}} = (E_{\mathrm{loss,Rv}} + E_{\mathrm{loss,Rc}}) \times N_{\mathrm{day}} \\ E_{\mathrm{loss,T,day}} = E_{\mathrm{loss,Tul}} + (E_{\mathrm{loss,Tc}} + E_{\mathrm{loss,Tv}}) \times N_{\mathrm{day}} \end{cases} \tag{14}$$

$E_{\mathrm{loss,dd,day}}$, $E_{\mathrm{loss,sc,day}}$, $E_{\mathrm{loss,boost,day}}$, $E_{\mathrm{loss,R,day}}$ and $E_{\mathrm{loss,dd,day}}$, are the total daily loss of step-down DC/DC, ground energy storage device, boost DC/DC, rectifier, and transformer, respectively;

The total daily loss is:

$$E_{\mathrm{loss,day}} = E_{\mathrm{loss,dd,day}} + E_{\mathrm{loss,bc,day}} + E_{\mathrm{loss,boost,day}} + E_{\mathrm{loss,R,day}} + E_{\mathrm{loss,T,day}} \tag{15}$$

The efficiency of the daily average power supply is

$$\eta_{\mathrm{stop}} = \frac{N_{\mathrm{day}} \times E_{\mathrm{op}}}{E_{\mathrm{loss,day}} + N_{\mathrm{day}} \times E_{\mathrm{op}}} \tag{16}$$

According to the above formula, the weekly average power supply efficiency in summer and autumn is

$$\begin{cases} \eta_{\mathrm{sum,week}} = \frac{E_{\mathrm{op,sum}} \times (N_{\mathrm{wd}} \times 5 + N_{\mathrm{wd}} \times 2)}{E_{\mathrm{op,sum}} \times (N_{\mathrm{wd}} \times 5 + N_{\mathrm{wd}} \times 2) + E_{\mathrm{loss,wd,sum}} \times 5 + E_{\mathrm{loss,wk,sum}} \times 2} \\ \eta_{\mathrm{aut,week}} = \frac{E_{\mathrm{op,aut}} \times (N_{\mathrm{wd}} \times 5 + N_{\mathrm{wd}} \times 2)}{E_{\mathrm{op,aut}} \times (N_{\mathrm{wd}} \times 5 + N_{\mathrm{wd}} \times 2) + E_{\mathrm{loss,wd,aut}} \times 5 + E_{\mathrm{loss,wk,aut}} \times 2} \end{cases} \tag{17}$$

N_{wd} and N_{wk} are the daily total number of departure pairs on working days and rest days, respectively; $E_{\mathrm{op,sum}}$ and $E_{\mathrm{op,aut}}$ are the charging energy consumption per pair in summer and autumn, respectively; $E_{\mathrm{loss,wd,sum}}$ and $E_{\mathrm{loss,wk,aut}}$ are the total daily loss of summer working days and rest days, respectively; $E_{\mathrm{loss,wd,aut}}$ and $E_{\mathrm{loss,wk,aut}}$ are the total daily loss of autumn working days and rest days, respectively.

To meet the design goal (increase the power supply efficiency by 5%), it can be reversed that the energy efficiency of the ground energy storage device is at least 93.48% (which can be easily achieved considering the charge power of 504 kW,). Table 6 shows the average power supply efficiency of the energy storage power supply system in each season.

Table 6. The comparison of average power supply efficiency.

Average Power Supply Efficiency	Original Power Supply System (%)	Energy Storage Power Supply System (%)	Growth Rate (%)
Summer	89.05	92.98	4.41
Autumn	83.22	87.92	5.65
Daily	86.14	90.45	5.00

3.2. Design of Ground Energy Storage Device

During working hours, the ground energy storage device outputs high-power electric energy stored when the train enters the station to meet the demands for fast charge. After the train leaves the station, the energy storage device is charged by boosted DC/DC with low power until fully charged. Therefore, the no-load loss of grid side transformer is reduced when the train is withdrawn from operation at night.

3.2.1. Capacity Configuration

A 60,000 F capacitive monomer is used. The main parameters are as follows: the voltage working range is 2.4~3.5 V, the maximum working current is 100 A (10 C), the energy density is 40 Wh/kg, the power density is 2314 W/kg, the internal resistance is 0.3 mΩ (30 °C), and the cycle lifetime is 30,000 times. To evaluate the efficiency of the capacitive monomer in actual working conditions, the energy efficiency at different discharge currents is tested as follows:

(1) Charged to 3.45 V at 35 A and discharged at 110 A for 50 s, energy efficiency averaged 96.60%;
(2) Charged to 3.45 V at 35 A and discharged at 140A for 50 s, energy efficiency averaged 96.20%;
(3) Charged to 3.45 V at 35 A and discharged at 170 A for 50 s, energy efficiency averaged 95.50%;
(4) Fully charged and fully discharged at 100 A, energy efficiency averaged 94.33%.

According to the results of the efficiency experiments, the pre-configured battery capacitor scheme is shown in Table 7.

Table 7. The battery capacitor configuration scheme.

Parallel Connection	Series Connection	Voltage (V)	Monomer Charge–Discharge Current (A)	Monomer Discharge Energy (Wh)	Voltage Test
2	408	1400	<55.140	10.42 (3.185~3.45 V)	Satisfied
	384	1300	<55.151	11.07 (3.180~3.45 V)	Satisfied
	348	1200	<55.163	12.22 (2.816~3.45 V)	Not satisfied
	324	1100	55.178	13.12 (2.764~3.45 V)	Not satisfied
3	408	1400	<35.93	6.95 (3.214~3.45 V)	Satisfied
	384	1300	<35.100	7.38 (3.211~3.45 V)	Satisfied
	348	1200	<35.108	8.15 (3.205~3.45 V)	Satisfied
	324	1100	35.118	8.75 (3.199~3.45 V)	Satisfied

Based on the performance of the 60,000 F monomer: the standard charge and discharge current is 100 A, the maximum working current is 200 A under forced heat dissipation conditions, and the pulse current is 300 A (30 s). If the 2-parallel scheme is configured, the discharge current of the monomer is close to 200 A or even exceeds 200 A. Then the operation target can only be met under the forced heat dissipation condition. Therefore, considering the system efficiency and system heat dissipation requirement after the capacitive monomers are assembled, the 1200 V/348S3P is finally selected. This configuration not only achieves the goal of improving efficiency, but also maintains considerable capacity retention and energy efficiency after a long-term decline.

3.2.2. Circuit Configuration

The ground energy storage device is mainly composed of energy storage cabinets (2 sets are connected in series by cables), modules (58 sets), voltage equalization unit, main control unit, control and protection circuit, heat dissipation system, etc. The voltage equalization unit and the main control unit constitute the CMS. The main parameters are shown in Table 8.

Table 8. The system parameters of the ground energy storage device.

Parameter	Value
Monomer	3.6 V/60,000 F
Total system power (kWh)	52.2
Rated voltage (VDC)	1252.8
Optimal working voltage (VDC)	835.3~1218
Standard charge–discharge current (A)	300
Pulse current@30 s (A)	900

The supercapacitor module is composed of monomers in series and parallel (6S3P). In addition, the module is mainly composed of 18 supercapacitor monomers, circuits for balancing, and structural parts. The balancing circuit monitors the information such as the voltage of each parallel node and the temperature of the module, and reports it to the main control system through the communication bus. Then the main control system processes the data and issues corresponding action commands. In addition, the circuit board can equalize the voltage of multiple monomers at the same time, which can effectively reduce the voltage difference between cells and improve capacity utilization.

3.2.3. Control Strategy

The capacitor management system (CMS) is mainly used to monitor the supercapacitor energy storage system, with functions such as system current acquisition, total voltage acquisition, and leakage detection. When the energy storage system is in fault, it will alarm and notify the upper-level management system. Then the system can reduce power or stop running to ensure safety, more specifically:

(1) System current: the bus current sensed by the Hall sensor. The discharge direction of the system denotes a positive value, and the charging direction denotes a negative value.
(2) System voltage: the total system voltage collected through the high-voltage sample line in the bus, different from the accumulated voltage obtained by monitoring the monomer. When the high-voltage sample line in a bus is recognized as invalid, the system will switch to show the accumulated voltage of the monomers and report the fault.
(3) The highest voltage of a single cell: the highest parallel node voltage in the energy storage system, which determines the charging limit of the system.
(4) The maximum temperature of the module: the highest temperature displayed by all temperature sensors of the energy storage system. When the temperature is too high, the system will alarm to prevent thermal failure.

3.3. Working Mode

The working mode of the collaborative energy storage power supply is as follows:

Step1: Read the voltage value (U) of the current power supply rail through the voltage sensor for status judgment;
Step2: If U = 0, charge the energy storage device at a preset low power by a boost DC/DC converter; if U $\neq$ 0, check whether the disconnector of the current power supply system is closed;
Step3: If the disconnector is closed, continue to perform step 2; if not, then close the disconnector of the power supply rail currently connected to the vehicle to be charged;

Step4: Collect the electric energy from the boost DC/DC converter and the energy storage device through a step-down DC/DC converter and transfer the obtained energy to the vehicle;
Step5: Check through the voltage sensor whether the current voltage at the supply rail reaches the full voltage;
Step6: If yes, disconnect the disconnector at the power supply rail.

3.4. Energy Efficiency Analysis before and after Upgrade

Combined with recent operation data, upgrading the power supply system put forward performance requirements of crucial equipment in the line. Calculation analysis shows a 5.26% expected increase in power supply efficiency. By collecting the input energy consumption of the transformer and the output energy consumption of the buck DC/DC, the effectiveness of the efficiency improvement of the power supply system is verified. The comparison results are shown in Table 9.

Table 9. The AC and DC power before and after upgrade.

Electricity Consumption (6 Months)	Before	After
AC (kWh)	85,200	77,910
DC (kWh)	73,633	71,429
Average AC/DC conversion rate (%)	86.42	91.68

After the upgrade, the energy consumption of the system is reduced, and the energy efficiency is increased by 5.26%, which meets the design requirements. The supercapacitor storages and efficiency test equipment is shown in Figure 7.

(**a**) (**b**)

Figure 7. Efficiency test of supercapacitor storage. (**a**) Supercapacitor storage. (**b**) Efficiency test equipment.

4. Conclusions

To realize an efficient, reliable and economical power supply system of energy storage tram based on supercapacitors, this paper designs an energy storage collaborative power supply system and conducts practical verification on a line in field operation.

(1) The charging topology and main parameters of the collaborative energy storage system are designed, and the efficiency chain model and load characteristics of the charging system are analyzed. The power supply topology of the ground energy storage system is designed based on the supercapacitor and the boost DC/DC converter, which have good flexibility to realize the upgrade of the existing power supply system.
(2) The proposed system effectively reduces the transformer capacity requirement, the no-load loss, and load loss. After adding supercapacitor energy storage, the transformer

can charge the supercapacitor when the vehicle enters the station; after the vehicle enters the station, the transformer maintains the same charge power with the ground supercapacitor providing additional power.

(3) Based on the system power flow transfer, the system efficiency expression is obtained, and the topology performance is theoretically analyzed. Calculation of energy consumption data demonstrates that the energy efficiency of the energy storage collaborative power supply system has been significantly improved by 5%.

(4) The proposed topology can also reduce the exclusive requirements for front-end grid power supply, suitable for some areas without 10 kV dedicated lines or scenarios for new energy power supply. Meanwhile, it provides a reference for subsequent research, such as on canceling the rectifier and charging the energy storage system on the ground directly through AC/DC.

Author Contributions: Conceptualization, Y.D. (Yibo Deng) and C.L. (Chengmin Li).; methodology, Y.D. (Yibo Deng) and Y.D. (Yan Deng); software, Y.D. (Yibo Deng) and Y.C.; validation, Y.D. (Yibo Deng) and T.C.; formal analysis, Y.D. (Yibo Deng) and C.L. (Chengmin Li).; investigation, Y.D. (Yibo Deng) and S.F.; resources, C.L. (Chushan Li) and Y.D. (Yan Deng); data curation, Y.D. (Yibo Deng), T.C. and C.L. (Chengmin Li); writing—original draft preparation, Y.D. (Yibo Deng) and S.F.; writing—review and editing, C.L. (Chengmin Li), C.L. (Chushan Li) and Y.D. (Yan Deng); visualization, Y.D. (Yibo Deng) and S.F.; supervision, C.L. (Chengmin Li), C.L. (Chushan Li) and Y.D. (Yan Deng); project administration, Y.D. (Yibo Deng), T.C. and C.L. (Chengmin Li); funding acquisition, Y.D. (Yibo Deng) and C.L. (Chushan Li). All authors have read and agreed to the published version of the manuscript.

Funding: This research was funded by the National Key R&D Program of China, grant number 2017YFB1201004.

Data Availability Statement: The data presented in this study are available on request from the corresponding author.

Conflicts of Interest: The authors declare no conflict of interest.

Nomenclature

D_{peak}	Number of departures per hour
E_{ch}	Energy consumption of ground energy storage during each charging in case of coordinated power supply by supercapacitor
E_{op}	Charging quantity of on-board energy storage system of each pair of vehicles
$E_{loss,dd}$	Energy loss of step-down DC/DC during each charging in case of coordinated power supply by supercapacitor
$E_{loss,Tv}$	Energy loss of transformer during each charging in case of coordinated power supply by supercapacitor
$E_{loss,Rv}$	Energy loss of rectifier during each charging in case of coordinated power supply by supercapacitor
$E_{loss,ddv}$	Energy loss of boost DC/DC during each charging in case of coordinated power supply by supercapacitor
$E_{loss,sc}$	Energy loss of ground energy storage during each charging in case of coordinated power supply by supercapacitor
$E_{loss,ddc}$	Every time the ground energy storage system is replenished, the energy loss of the boost DC/DC
$E_{loss,Rc}$	Every time the ground energy storage system is replenished, the energy loss of the rectifier
$E_{loss,Tc}$	Every time the ground energy storage system is replenished, the energy loss of the transformer
$E_{loss,Tul}$	No-load loss of transformer

$E_{loss,dd,day}$	Total daily loss of step-down DC/DC
$E_{loss,sc,day}$	Total daily loss of ground energy storage system
$E_{loss,boost,day}$	Total daily loss of boost DC/DC
$E_{loss,R,day}$	Total daily loss of rectifier
$E_{loss,T,dayv}$	Total daily loss of transformer
$E_{loss,wd,sum}$	Total daily loss of summer working days
$E_{loss,wk,aut}$	Total daily loss of summer rest days
$E_{loss,wd,aut}$	Total daily loss of autumn working days
$E_{loss,wk,aut}$	Total daily loss of autumn rest days
$E_{loss,day}$	Total daily loss
$E_{op,sum}$	Charging energy consumption per pair in summer
$E_{op,aut}$	Charging energy consumption per pair in autumn
N_{day}	Total number of daily departures
N_{wd}	Daily total number of departure pairs on working days
N_{wk}	Daily total number of departure pairs on rest days
P_{ch}	Rated power of charger
T_{rech}	The charge time of a single cycle of the transformer
t_{charge}	Charging time
$t_{interval}$	Charging interval time
η	The supercapacitor energy efficiency of the collaborative energy storage power charging system
η_{line}	The distribution network efficiency
η_{OESS}	The on-board energy storage system efficiency
η_{t0}	The transformer efficiency when the direct charging system during charging period
η_{r0}	The rectifier efficiency when the direct charging system during charging period
η_{bk0}	The step-down DC/DC efficiency when the direct charging system during charging period
η_{t1}	The transformer efficiency when the collaborative energy storage charging system during idle period
η_{r1}	The rectifier efficiency when the collaborative energy storage charging system during idle period
η_{bt1}	The boost DC/DC efficiency when the collaborative energy storage charging system during idle period
η_{c1}	The energy storage system charging efficiency when the collaborative energy storage charging system during idle period
η_{bk1}	The step-down DC/DC efficiency when the collaborative energy storage charging system during idle period
η_{t2}	The transformer efficiency when the collaborative energy storage charging system during charging period
η_{r2}	The rectifier efficiency when the collaborative energy storage charging system during charging period
η_{bt2}	The boost DC/DC efficiency when the collaborative energy storage charging system during charging period
η_{c2}	The energy storage system discharge efficiency when the collaborative energy storage charging system during charging period
η_{bk2}	The step-down DC/DC efficiency when the collaborative energy storage charging system during charging period
η_{Tch}	Efficiency of a single cycle of the transformer
η_{stop}	Daily average power supply efficiency
$\eta_{sum,week}$	Average weekly power supply efficiency in summer
$\eta_{aut,week}$	Average weekly power supply efficiency in autumn

References

1. Yang, Y.; Chen, Z.J. Research and Development of Energy Storage Electric Traction Light Rail Transport. *Electr. Locomot. Mass Transit Veh.* **2012**, *35*, 5–10+20.
2. Tian, W.; Chang, P.; Lin, C. Analysis of Tram Charging Device under Different Power Supply Networks. *Mod. Urban Transit* **2018**, *8*, 13–15.
3. Radaš, I.; Župan, I.; Šunde, V.; Ban, Ž. Route Profile Dependent Tram Regenerative Braking Algorithm with Reduced Impact on the Supply Network. *Energies* **2021**, *14*, 2411–2432. [CrossRef]
4. He, Z.; Zhao, Y.; Zhu, D.; Su, X. Research on the Charging Device of Energy-storage Tram for Parking-lot. *Electr. Drive* **2018**, *48*, 70–74.
5. Zhang, G.; Li, Q.; Chen, W.; Meng, X.; Deng, H. A coupled power-voltage equilibrium strategy based on droop control for fuel cell/battery/supercapacitor hybrid tramway. *Int. J. Hydrog. Energy* **2019**, *44*, 19370–19383. [CrossRef]
6. Yang, J.; Xu, X.; Peng, Y.; Zhang, J.; Song, P. Modeling and optimal energy management strategy for a catenary-battery-ultracapacitor based hybrid tramway. *Energy* **2019**, *183*, 1123–1135. [CrossRef]
7. Wei, S.; Murgovski, N.; Jiang, J.; Hu, X.; Zhang, W.; Zhang, C. Stochastic optimization of a stationary energy storage system for a catenary-free tramline. *Appl. Energy* **2020**, *280*, 115711. [CrossRef]
8. Oukkacha, I.; Sarr, C.T.; Camara, M.B.; Dakyo, B.; Parédé, J.Y. Energetic Performances Booster for Electric Vehicle Applications Using Transient Power Control and Supercapacitors-Batteries/Fuel Cell. *Energies* **2021**, *14*, 2251–2272. [CrossRef]
9. Wei, S.; Jiang, J.; Cheng, L. Optimal Sizing Model of the Energy Storage Type Tramway Considering the Integration of on-Board Energy Storage and off-Board Energy Supply. *Trans. China Electrotech. Soc.* **2019**, *34*, 229–238.
10. Wang, B.; Yang, Z.; Lin, F.; Zhao, W. Study on Optimization of Capacity Configuration of Stationary Super Capacitor Storage System for Improving Energy Efficiency and Voltage Profile. *J. China Railw. Soc.* **2016**, *38*, 45–52.
11. Su, X.; Zhu, L.; Tian, W. Research on Control for Tram Charging Device Based on Super-capacitor. *Power Electron.* **2016**, *50*, 60–62.
12. Di Noia, L.P.; Genduso, F.; Miceli, R.; Rizzo, R. Optimal integration of hybrid supercapacitor and IPT system for a free-catenary tramway. *IEEE Trans. Ind. Appl.* **2018**, *55*, 794–801. [CrossRef]
13. Li, H.; Peng, J.; He, J.; Zhou, R.; Huang, Z.; Pan, J. A cooperative charging protocol for onboard supercapacitors of catenary-free trams. *IEEE Trans. Control Syst. Technol.* **2017**, *26*, 1219–1232. [CrossRef]
14. Şahin, M.E.; Blaabjerg, F.; Sangwongwanich, A. A comprehensive review on supercapacitor applications and developments. *Energies* **2022**, *15*, 674–699. [CrossRef]
15. Guo, C.; Zhang, A.; Zhang, H. Model Predictive Control for Tram Charging and its Semi-physical Experimental Platform Design. *J. Power Electron.* **2018**, *18*, 1771–1779.
16. Herrera, V.; Milo, A.; Gaztañaga, H.; Etxeberria-Otadui, I.; Villarreal, I.; Camblong, H. Adaptive energy management strategy and optimal sizing applied on a battery-supercapacitor based tramway. *Appl. Energy* **2016**, *169*, 831–845. [CrossRef]
17. Chang, P.; Tian, W.; Lin, C. Research on Energy Storage Type Charging Devices for Modern Trams. *Electr. Autom.* **2019**, *41*, 102–104.
18. Xie, Y.; Bai, Y. Overall Capacity Allocation of Energy Storage Tram with Ground Charging Piles. *Energy Storage Sci. Technol.* **2021**, *10*, 1388–1399.
19. Wu, W.; Hu, J.; Yang, H.; Feng, A. Research on a 2 MW Timcar Charqlng Device. *Electr. Veh. Technol.* **2020**, *42*, 47–49+101.
20. Rong, L.; Tian, W.; Sun, Z. Research on Charging Device of Super Capacitor Tram. *Power Electron.* **2020**, *54*, 11–14.
21. Zahng, W.; Tao, Z.; Luo, Q.; Zheng, R. Development of an Isolated Charing Device for Energy-storage Trams. *Power Electron.* **2021**, *55*, 34–36+48.
22. Jin, X.; Chen, Y. Study on Optimization Design of Fast Energy Storage in the Charging Device of the Tram. *Comput. Simul.* **2017**, *34*, 151–155+225.
23. Yang, J.B.; Xu, X.H.; Peng, Y.Q. Optimal Parameter Matching of Hybrid Energy Storage System Based on NSGA-II Algorithm for Energy Storage Type Tram. *J. Mech. Eng.* **2020**, *56*, 181–189.
24. Ciccarelli, F.; Iannuzzi, D.; Kondo, K.; Fratelli, L. Line-voltage control based on wayside energy storage systems for tramway networks. *IEEE Trans. Power Electron.* **2015**, *31*, 884–899. [CrossRef]
25. Zhou, Y.; Zhang, L.; Xiu, S.; Hao, W. Design and Analysis of Platform Shielding for Wireless Charging Tram. *IEEE Access* **2019**, *7*, 129443–129451. [CrossRef]
26. Yan, Y.; Li, Q.; Chen, W.; Su, B.; Liu, J.; Ma, L. Optimal energy management and control in multimode equivalent energy consumption of fuel cell/supercapacitor of hybrid electric tram. *IEEE Trans. Ind. Electron.* **2018**, *66*, 6065–6076. [CrossRef]
27. Qiu, L.; Wang, X.; Tao, Z. Analysis and Protection of Output Over-voltage for Energy Storage Tram Charging Device. *Urban Mass Transit* **2020**, *23*, 72–74.
28. Yang, L.; Wei, S. Improvement of Ground Power Supply Scheme for Energy Storage Tram. *Electr. Locomot. Mass Transit Veh.* **2020**, *43*, 56–60+64.

29. Zhang, W.; Wen, W. Ground Charging System for Energy Storage Modern Tram. *Electr. Locomot. Mass Transit Veh.* **2015**, *38*, 30–32.
30. Chen, W.; Shi, F.; Dai, C.; An, Q.; Liu, Y.; Liu, Y. Energy Management Strategy of Hybrid Tram Based on Dynamic Degree of Hybrid. *J. Southwest Jiaotong Univ.* **2020**, *55*, 409–416.